Survival Analysis with Machine Learning for Predicting Li-ion Battery Remaining Useful Life

Jingyuan Xue^{1,2,†} Longfei Wei^{1,3,†} Fang Sheng^{1,3,4} Yuxin Gao^{3,5} Jianfei Zhang^{1,3,*}

¹ThinkX, Canada ²Eve Energy, China ³MedicineX, Canada ⁴University of Toronto, Canada ⁵Southeast University, China

ABSTRACT

The accurate prediction of RUL for lithium-ion batteries is crucial for enhancing the reliability and longevity of energy storage systems. Traditional methods for RUL prediction often struggle with issues such as data sparsity, varying battery chemistries, and the inability to capture complex degradation patterns over time. In this study, we propose a survival analysis-based framework combined with deep learning models to predict the RUL of lithium-ion batteries. Specifically, we utilize five advanced models: the Cox-type models (Cox, CoxPH, and CoxTime) and two machine-learning-based models (DeepHit and MTLR). These models address the challenges of accurate RUL estimation by transforming raw time-series battery data into survival data, including key degradation indicators such as voltage, current, and internal resistance. Advanced feature extraction techniques enhance the model's robustness in diverse real-world scenarios, including varying charging conditions and battery chemistries. Our models are tested using 10-fold crossvalidation, ensuring generalizability and minimizing overfitting. Experimental results show that our survival-based framework significantly improves RUL prediction accuracy compared to traditional methods, providing a reliable tool for battery management and maintenance optimization. This study contributes to the advancement of predictive maintenance in battery technology, offering valuable insights for both researchers and industry practitioners aiming to enhance the operational lifespan of lithium-ion batteries. The source code for this work is available to the public at https://github.com/thinkxca/rul.

1 Introduction

In industrial sectors, ensuring the long-term reliability and continuous operation of equipment is crucial for maintaining production efficiency. However, equipment aging and failure are inevitable, making predictive maintenance essential. Traditional time-based or usage-based maintenance strategies often lead to inefficiencies. For example, over-maintenance wastes resources

[†]These authors contributed equally

^{*}Corresponding author: zhang@thinkx.ca

and increases costs by replacing components prematurely. Lack of maintenance increases failure risks, causing production stoppages, higher repair costs, and potential safety hazards. To address these challenges, remaining useful life (RUL) prediction has emerged as a transformative approach, enabling optimized, condition-based maintenance strategies that enhance reliability and cost-efficiency. As the core energy source in electric vehicles (EVs), lithium-ion (Li-ion) batteries play a pivotal role in the industry's viability. Their reliability and longevity directly impact EV adoption and lifecycle costs. RUL prediction - i.e., estimating the remaining cycles or time before a battery reaches its end-of-life (typically at 70–80% of initial capacity) - is crucial for 1) predictive maintenance to prevent unexpected failures; 2) extending battery lifespan and improving EV durability; and 3) reducing operational costs and enhancing user experience.

However, accurate battery RUL prediction is challenging due to the following reasons: 1) complex, nonlinear degradation mechanisms – Battery aging involves multiple interacting factors (e.g., SEI growth, lithium plating, active material loss) that vary with temperature, charging rates, and depth of discharge, leading to highly stochastic degradation patterns; 2) limited generalization across battery types and conditions – Variability in battery chemistries, manufacturing inconsistencies, and real-world usage further complicates modeling across diverse scenarios; 3) scarcity of complete end-of-life data – Battery aging tests span 6 months to 2 years, making data collection costly and time-consuming. Many batteries retain functional capacity by the test's end, limiting the availability of true end-of-life data. Traditional extrapolation methods struggle with these challenges, often relying on assumptions that do not hold in real-world applications. This underscores the need for advanced, data-driven approaches to improve the accuracy, robustness, and generalizability of RUL prediction models.

Accurately predicting RUL of Li-ion batteries requires effective modeling of their degradation patterns. Since battery aging is a progressive and uncertain process, traditional regression models that provide fixed-point estimates often fail to capture the probabilistic nature of degradation. Survival analysis is designed to handle time-to-event data, offering a more flexible and informative approach for battery RUL prediction where battery failure is the event of interest (i.e., time-to-failure prediction). Unlike conventional regression models, survival models offer probabilistic insights – Instead of predicting a single failure point, survival models estimate failure probabilities over time using survival functions and hazard rates. Early-cycle inference – Survival models can efficiently leverage early-stage degradation data to infer long-term failure risks, reducing the time required for RUL estimation. Dynamic maintenance strategies – By continuously updating predictions based on evolving battery health indicators, survival analysis enables adaptive warranty adjustments and predictive maintenance. Traditional survival models, such as Kaplan-Meier estimators (Mo et al., 2016) and Weibull distributions (Deng et al., 2023), have been used to describe battery degradation processes. However, these models often impose restrictive assumptions (e.g., proportional hazards), limiting their adaptability to real-world battery aging. Recent advancements in machine learning methods have significantly improved time-to-failure prediction by overcoming these limitations (Zhang et al., 2020).

Extracting meaningful features from battery time-series data is crucial for modeling degradation. Traditional methods, such as statistical measures and hand-crafted features, struggle to capture the complex nonlinear interactions governing battery aging. To address this, we employ path signatures to capture high-order interactions and temporal dependencies, providing a robust representation for

survival modeling. and the battery health indicators – features such as capacity degradation rates, changes in internal resistance, and voltage profiles over time, derived through statistical and machine learning-based techniques. After feature extraction, each battery sample is associated with: 1) Time-to-failure – the number of cycles or time until failure, and 2) censoring status – whether the battery has failed or is still operational at the last observation point.

This study presents a survival analysis framework for Li-ion battery Remaining Useful Life (RUL) prediction, emphasizing its generalizability across different battery chemistries and operating conditions. Unlike traditional methods that primarily focus on end-of-life prediction, our approach enables real-time RUL estimation while addressing key challenges such as data sparsity and variability in real-world applications. To optimize RUL prediction, we enhance feature representation by embedding cell voltage trajectory signatures as shared inputs. Additionally, we introduce cycle-adaptive temporal discretization to improve time resolution in survival modeling. To mitigate overfitting, we apply early stopping regularization based on capacity fade characteristics. By integrating survival analysis with deep learning, this study aims to enhance the accuracy, reliability, and generalizability of battery RUL predictions. The proposed methodology provides a robust framework for predictive maintenance and battery lifecycle optimization, contributing to advancements in battery management systems for electric vehicles and other critical applications.

- A novel survival analysis framework integrating robust feature extraction techniques, enhancing adaptability and reliability across diverse datasets.
- Comprehensive model evaluation across various real-world scenarios, including low-data environments and different charging conditions.
- Actionable insights for battery manufacturers and engineers, enabling improved battery design and dynamic maintenance strategies.

2 Related Work

RUL prediction methods are generally fall into three groups: model-based methods, data-driven methods, and hybrid methods (Hu et al., 2020).

2.1 Model-based Methods

Model-based methods play a crucial role in battery health monitoring and RUL prediction by simulating battery behavior using physical, electrochemical, or equivalent circuit models (Ahwiadi and Wang, 2025). These models provide insights into degradation mechanisms, operational impacts, and dynamic system behaviors (Li et al., 2014). By integrating theoretical principles with practical adaptability, model-based approaches enhance battery management system (BMS) performance and ensure long-term reliability. Model-based methods adapt well to environmental changes such as load fluctuations and temperature variations, increasing their real-world applicability. When coupled with uncertainty quantification, these methods offer robust state estimation and RUL prediction under dynamic conditions (Kordestani et al., 2019). Common approaches include:

• **Electrochemical Models**: Simulate processes like ion transport and SEI formation, providing detailed degradation insights. However, high computational costs limit real-time applications.

- **Semi-Empirical Models**: Combine experimental data with simplified physical equations, enabling real-time SOH and RUL estimation but with reduced accuracy under extreme conditions.
- Equivalent Circuit Models (ECM): Use electrical components (resistors, capacitors) to approximate battery behavior. They are computationally efficient but less accurate under high charge/discharge rates.

Several studies improve model-based RUL prediction. (Mo et al., 2016) proposed integrating Kalman filtering and particle swarm optimization (PSO) into particle filters (PF) to refine RUL estimation, validated on the NASA battery dataset. (Duan et al., 2020) introduced an extended Kalman particle filter (EKPF) that optimizes PF sampling for enhanced accuracy. (Al-Greer et al., 2023) developed a physics-based prognostics framework combining a single particle model (SPM) with a smooth particle filter (SPF) to capture degradation mechanisms more effectively.

2.2 Data-driven Methods

Data-driven approaches leverage machine learning to directly learn nonlinear degradation behaviors from historical and real-time data (Li et al., 2024). Traditional methods include:

- **Support Vector Regression (SVR)**: High accuracy but sensitive to parameter selection and lacks uncertainty quantification.
- **Relevance Vector Machine (RVM)**: Provides probabilistic outputs, useful for reliability-critical applications, albeit with higher computational costs.
- Gaussian Process Regression (GPR): Models nonlinear relationships and provides confidence intervals but suffers from scalability issues.

Soft computing techniques offer adaptability to complex degradation patterns. Artificial Neural Networks (ANNs) excel at extracting nonlinear relationships but require high computational power and risk overfitting. Adaptive Neuro-Fuzzy Inference Systems (ANFIS) integrate neural learning with fuzzy logic, enhancing interpretability while handling uncertainties, though performance depends on initial rule selection. Recent advances include (Xing et al., 2023), which applied Principal Component Analysis (PCA) to extract health indicators (HI) and improved Gaussian Process Regression (IGPR) for enhanced RUL prediction. (Reza et al., 2024) reviewed RUL prediction challenges for electric vehicles, emphasizing the role of battery management systems (BMS) and the need for improved feature extraction and hyperparameter tuning.

2.3 Hybrid Methods

Hybrid methods integrate model-based and data-driven techniques to enhance accuracy, reliability, and adaptability in RUL prediction. They effectively handle varying operational conditions, capture nonlinear degradation patterns, and mitigate data limitations. By combining physics-based models with machine learning, hybrid approaches improve predictive performance even with incomplete or low-quality data. For example, (Ren et al., 2024) proposed a fusion method combining an electrochemical-thermal model (ECT) with an unscented Kalman filter (UKF) for RUL prediction. The model incorporated a pseudo two-dimensional (P2D) electrochemical model, a 3D thermal model, and SEI formation dynamics. UKF iteratively updated parameters, improving accuracy

over time. Hybrid methods are increasingly recognized as a key solution for advancing battery health monitoring and RUL prediction, balancing computational efficiency with predictive robustness.

3 Data Transformation

The key to applying survival analysis to the RUL prediction is the transformation that transfers battery time-series into time-to-failure data. Time-series data typically consist of sequential observations, such as battery voltage, capacity, and internal resistance, collected at regular intervals. In the context of battery RUL prediction, these time-series measurements provide valuable information about the degradation state of the battery over time. To convert this time-series data into time-to-failure data, we need to associate each battery's performance trajectory with the survival analysis framework. In the survival analysis context, an "event" refers to the occurrence of the battery's failure, which is defined when the battery's capacity falls below a predetermined threshold (e.g., 70-80% of its initial capacity). The time-to-failure is the number of cycles or time until this failure occurs. Batteries that have not yet failed at the time of data collection are considered censored data. These batteries may continue to function, and their failure times are unknown. For these instances, time-to-failure data is represented by the last observed time point before the battery reaches the threshold or is removed from the dataset due to some other reason (e.g., maintenance, failure in testing).

3.1 Path-Signature-based Transformation

This transformation converts the time-series voltage data into a geometric trajectory that captures the temporal evolution of battery performance. Given the voltage V(t) at time t during charging or discharging period, we represent the time-dependent voltage at the time $t \in [t_0, t_\infty]$ as a sequence $V(t) = (v_1(t), v_2(t), \dots, v_M(t)) \in \mathbb{R}^M$. The k-depth truncated signature is a sequence of iterated integrals that capture the interactions along the sequence, i.e.,

$$S_{k}[V(t)] = \left(\sigma_{1}[V(t)], \sigma_{2}[V(t)], \sigma_{1,1}[V(t)], \sigma_{1,2}[V(t)], \sigma_{2,1}[V(t)], \dots, \sigma_{m_{1},\dots,m_{k}}[V(t)]\right)$$

$$\sigma_{k}[V(t)] = \int_{t_{0} < t_{k} < t} \dots \int_{t_{0} < t_{1} < t_{2}} dV^{(m_{1})}(t_{1}) \dots dV^{(m_{k})}(t_{k}) \qquad m_{1}, \dots, m_{k} \in \{1, 2, \dots, M\}$$

Here, $\sigma_k[V(t)]$ denotes the integrated integrals at depth k. The $\sigma_1[V(t)]$ represents the total elapsed time and the total voltage change, while other signatures capture pairwise interactions.

For each cell's voltage curve, the feature for each battery is constructed as $\mathbf{x}(t) = S_k[V(t)]$, where $\mathbf{x}(t)$ represents the time-varying voltage for a cell. By stacking the feature vectors of all N batteries, we obtain the feature matrix:

$$\mathbf{X} = \left(S_k[S_k[V(t)]_1], S_k[S_k[V(t)]_2], \dots, S_k[S_k[V(t)]_{m_1, \dots, m_k}] \right) \in \mathbb{R}^{N \times (2^{(k+1)} - 2)}$$

By concatenating the signatures across all batteries to build a high-dimensional data representation that effectively encodes temporal dependencies and non-linear interactions observed in the charging and discharging cycles. This approach effectively encodes the temporal and geometric features of the degradation process, enabling survival predictions despite variability in cycling conditions.

3.2 Time-to-Failure Data

For the sake of presentation in survival analysis, in what follows, denote by T a continuous nonnegative random variable representing time to failure. Given N batteries, let the triplet $(\mathbf{x}_i, \tau_i, \zeta_i)$ express the time-to-event labeled data for battery i, in which $\mathbf{x}_i \in \mathbb{R}^{2(2^k-1)}$. The censoring indicator outcome $\zeta_i = \mathbb{1}(T_i \leq C_i)$ equals 1 if battery capacity has dropped to 80% (or less) of its initial value and 0 otherwise. The scalar outcome time, τ_i , is either the minimum of time to event, T_i , and or the (right-)censoring time, C_i , that is,

$$\tau_i = \min\{T_i, C_i\} = \begin{cases} T_i, & \text{if } \zeta_i = 1 \text{ (i.e., Cell with a remaining capacity} \leq 80\%) \\ C_i, & \text{otherwise (i.e., Cell with a remaining capacity} > 80\%) \end{cases}$$

We shall assume without loss of generality that the individuals are ascendingly sorted according to observation, and T_i , C_i are conditionally independent given \mathbf{x}_i .

4 Survival Learning Machines

4.1 Cox-based Models

In this study, we focus on three Cox-type models, including the basic Cox proportional-hazards model, CoxPH (DeepSurv), and CoxTime model.

4.1.1 Cox Model

The Cox model (Cox, 1975) is widely adopted and considers that the hazard is determined by prognostic variables in a multiplicative manner:

$$h(t \mid \mathbf{x}) = h_0(t) \exp(f_{\text{Cox}}(\mathbf{x})) = h_0(t) \exp(\boldsymbol{\beta}^{\top} \mathbf{x}),$$

where $\beta \in \mathbb{R}^{2(2^k-1)}$ is a vector of regression coefficients (i.e., model parameters) describing how the hazard varies in response to the prognostic variables; $h_0(t)$ represents an arbitrary baseline hazard in the context of $\mathbf{x} = (0, \dots, 0)^{2(2^k-1)}$, describing how the risk of event per time unit changes over time. For any two individual batteries \mathbf{x}_1 and \mathbf{x}_2 , the hazard ratio is given by

$$\frac{h(t \mid \mathbf{x}_1)}{h(t \mid \mathbf{x}_2)} = \frac{h_0(t) \exp(\boldsymbol{\beta}^{\top} \mathbf{x}_1)}{h_0(t) \exp(\boldsymbol{\beta}^{\top} \mathbf{x}_2)} = \exp(\boldsymbol{\beta}^{\top} (\mathbf{x}_1 - \mathbf{x}_2)).$$

Since h_0 would be present in both nominator and denominator, it cancels out and thus no assumption about the shape of the baseline hazard needs to be made; this yields an efficient computation, where the hazard ratio is independent of the baseline hazard function. This is why the Cox model is called hazards-proportional. The key to learning a Cox model lies in finding the value of β that maximizes the probability of the observed data, i.e., maximize the likelihood of β given the observed data. As is generally the case, to estimate the likelihood we have to write the probability (or probability density) of the observed data as a function of β . The Cox model aims to maximize the partial likelihood in the form:

$$L(\boldsymbol{\beta}) = \prod_{i \in \mathcal{Z}_1} \frac{\Pr\left(\text{battery failed at } T_i; \boldsymbol{\beta}\right)}{\Pr\left(\text{all batteries survive at } T_i; \boldsymbol{\beta}\right)} = \prod_{i \in \mathcal{Z}_1} \frac{\exp(\boldsymbol{\beta}^\top \mathbf{x}_i)}{\sum_{j \in \mathcal{R}(T_i)} \exp(\boldsymbol{\beta}^\top \mathbf{x}_j)},$$

where $\mathcal{Z}_1 = \{i : \zeta_i = 1\}$ is the set of all batteries that failed during the observation period.

4.1.2 CoxTime

The proportionality assumption of the Cox model can be rather restrictive, and parameterizing the relative risk function with a neural net does not affect this constraint. A parametric approach, CoxTime (Kvamme et al., 2019), that does not require stratification and rebuilds a semi-parametric form of the Cox model, the relative risk function dependent on time is

$$L(\theta) = \frac{1}{|\mathcal{Z}_1|} \sum_{i \in \mathcal{Z}_1} \left(\sum_{j \in \mathcal{R}(T_i)} \exp\left(f_{\mathsf{Time}}(T_i, \mathbf{x}_j) - f_{\mathsf{Time}}(T_i, \mathbf{x}_i)\right) \right).$$

4.1.3 CoxPH

CoxPH (also DeepSurv) (Katzman et al., 2018) is a deep feed-forward neural network which predicts the effects of a battery's variables on their hazard rate parameterized by the weights of the network. The input to the network is a battery's baseline data \mathbf{x} . The hidden layers of the network consist of a fully-connected layer of nodes, followed by a dropout layer. The output of the network $f_{\text{DeepSurv}}(\mathbf{x},\theta)$ is a single node with a linear activation which estimates the log-risk function in the Cox model. It trains the network by setting the objective function to be the average negative log partial likelihood with regularization:

$$L(\theta) = \frac{1}{|\mathcal{Z}_1|} \sum_{i \in \mathcal{Z}_1} \left(\log \sum_{j \in \mathcal{R}(T_i)} \exp \left(f_{\text{DeepSurv}}(\mathbf{x}_j, \theta) \right) - f_{\text{DeepSurv}}(\mathbf{x}_i, \theta) \right).$$

4.2 Machine-Learning-based Models

Besides Cox-based models, we study two typical machine-learning-based survival models, i.e., DeepHit(Lee et al., 2018) and MTLR (Yu et al., 2011), which have been widely employed for most time-to-event prediction tasks.

4.2.1 DeepHit Model

DeepHit (Lee et al., 2018) considers time to be discrete, so to fit it to the continuous-time data sets, we discretize the event times with an equidistant grid between the smallest and largest duration in the training set. The number of discrete time-points is considered a hyperparameter. Assume time is discrete with $0 = \tau_0 < \tau_1 < \tau_2 \cdots < \tau_K$, the survival probability is

$$\Pr(T_k|\mathbf{x};W) = 1 - \sum_{j=1}^k \Pr(T_j = \tau_k; W).$$

DeepHit minimizes the loss

$$L(W) = \alpha L_1(W) + (1 - \alpha)L_2(W)$$

$$L_1(W) = -\sum_{i \in \mathcal{Z}_1} \zeta_i \cdot \log(\Pr(T_i = \tau_{e_i} | \mathbf{x}_i; W) + (1 - \zeta_i)\log(\Pr(T_i | \mathbf{x}_i; W)))$$

$$L_2(W) = \sum_{i \in \mathcal{Z}_1, j} \zeta_i \cdot \mathbb{1}(T_i < T_j) \exp\left(\sigma\left(\Pr(T_i | \mathbf{x}_i; W) - \Pr(T_i | \mathbf{x}_j; W)\right)\right)$$

4.2.2 MTLR

Multi-task learning regression (MTLR) (Yu et al., 2011) is a deep learning approach that models multiple tasks simultaneously by sharing representations across tasks. In the context of battery RUL prediction, MTLR can be used to predict the RUL for multiple batteries at once, learning shared features while predicting individual survival outcomes. MTLR can improve generalization by leveraging data from similar tasks, allowing for more accurate predictions when dealing with limited data. In MTLR, the objective is to minimize the loss function across multiple related tasks. For an individual indexed as $i \in \mathcal{Z}_0 = \{i : \zeta_i = 0\}$, possessing known battery health statuses denoted as $Y = (y_1, \ldots, y_K)$ at times $t_1 < \cdots < t_K$, along with associated variable values x ($\tau_V \le t_K$), we estimate the probability of observing Y through the utilization of generalized logistic regression.

$$\Pr(Y \mid \mathbf{X}; \mathbf{W})_{0} = \frac{\exp(\mathbf{W} * \mathbf{X} \cdot \mathbb{1}(\zeta \leq 0))}{\exp(\mathbf{W} * \mathbf{X}) \cdot \mathbf{1}}$$

$$\mathbf{W} * \mathbf{X} = (\mathbf{w}_{1} \cdot \mathbf{x}_{1}, \dots, \mathbf{w}_{D} \cdot \mathbf{x}_{D}) \in \mathbb{R}^{1 \times D}.$$
(1)

The regression coefficient \mathbf{W} serves to quantify the influence of factors and their recurrent measurements on the probability of an individual's event-free status. In this context, the coefficients \mathbf{w}_v signify the contribution of measurements denoted by D at the specific time τ_v . The summation of transformed measurements over V time instances is computed through a column-wise Hadamard product (Liu and Trenkler, 2008). The symbol \exp denotes the element-wise exponential operation applied to a matrix. To delve into event-free probabilities, we employ the lower triangular identity matrix denoted as $\mathbf{A} = (\alpha_1, \dots, \alpha_K) \in \mathbb{R}^{K \times K}$, where $\alpha_{ij} = 1$ if $i \geq j$ and 0 otherwise. This matrix aids us in investigating probabilities of remaining event-free. For individuals belonging to $\mathcal{Z}_1 = \{i : \zeta_i = 1\}$, who possess an unknown event time, their health statuses remain consistent before the given time stamp. Consequently,

$$\Pr(Y \mid \mathbf{X}; \mathbf{W})_{1} = \frac{\exp(\mathbf{W} * \mathbf{X} \mathbf{A} \cdot \mathbb{1}(\zeta \le 0)) \cdot \mathbf{1}}{\exp(\mathbf{W} * \mathbf{X} \mathbf{A}) \cdot \mathbf{1}}.$$
 (2)

The numerator represents the accumulation of the risks associated with the occurrence of target responses. To learn the matrix \mathbf{W} , we undertake minimization of the negative logarithm of the likelihood across all individuals through an expectation-maximization process. This involves suitable initialization and can be outlined as follows:

$$\min_{\mathbf{W}} P(\mathbf{W}) - \sum_{i \in \mathcal{Z}_0} \log(\Pr(Y_i|\mathbf{X}_i;\mathbf{W})_0) - \sum_{i \in \mathcal{Z}_1} \log(\Pr(Y_i|\mathbf{X}_i;\mathbf{W})_1).$$

The incorporation of the elastic-net penalty $P(\mathbf{W}) = \lambda_1 |\mathbf{W}|_1 + \lambda_2 |\mathbf{W}|_2^2$ into the loss function enhances its strong convexity, resulting in a unique minimum. To establish suitable values for the hyperparameters λ_1 and λ_2 , we rely on an independent validation set. The learning objective function exhibits strict convexity within the feasible domain $\mathbf{w}_k \in \mathbb{R}^D, \forall k$, ensuring a unique globally optimal solution.

5 Experiments

5.1 Data Collection and Pre-processing

The dataset used in this study is derived from the Toyota dataset, consisting of 373 Lithium Ferro Phosphate (LFP)/graphite A123 APR18650M1A cells. Each cell has an initial capacity of 1.1 Ah and an initial voltage of 3.3 V. The cells were cycled under strictly controlled experimental conditions, maintaining an ambient temperature of 30°C. The discharge process followed a constant-current-constant-voltage (CC-CV) protocol at a 4C rate until the voltage dropped to 2.0 V. Charging was performed in two stages: from 0-80% state of charge (SOC) using one of over 80 different charging policies, followed by a 1C CC-CV charge from 80-100% SOC, reaching a maximum voltage of 3.6 V. These variations introduced two major sources of variability: (1) protocol-to-protocol variability due to differences in charging policies, and (2) cell-to-cell variability arising from intrinsic differences among cells, even when cycled under identical discharge conditions.

The original column represents the actual number of cells in the downloaded Toyota dataset. Initially, 373 cells were included in the dataset. However, 11 cells were removed due to misclassification and noise issues. This resulted in a final count of 362 processed cells. We divided the dataset into four groups: the G1 group includes batches 1, 2, and 3, consisting of 129 samples; G2 includes batches 4 and 5, composed of 92 batteries; G3 includes batches 6 and 7, having 96 batteries; and the G4 group includes batch 8, composed of 45 samples. The dataset contains two types of cells based on their cycling termination: G1 (batches 1, 2, 3) and G4 (batch 8) were cycled to time-to-failure, defined as the point where the remaining capacity dropped to 80% of the initial capacity. In contrast, cells in the G2 (batches 4, 5) and G3 (batches 6, 7) groups were only cycled for a maximum of 120 cycles, resulting in censored data.

For each cell, voltage-time curves from the first 50 cycles were used as input, with separate signatures calculated for the charge and discharge phases. The k-depth balances model complexity, generalization, and computational cost, leading to more reliable and interpretable survival analysis results. Increasing the signature depth enhances the model's ability to capture complex interactions and higher-order dependencies. However, it also leads to an exponential growth in the dimensionality of the feature space, which can result in overfitting and increased computational cost. Choosing k=3 balances this trade-off by capturing sufficient non-linear interactions while maintaining a manageable feature dimension. We also evaluated the predictive performance of the survival models using signature depths k=2 and k=4. Results showed that k=3 provided the best trade-off between model accuracy and computational efficiency, with diminishing returns observed for higher depths. Lower-order signatures (e.g., k=2) failed to capture the non-linear temporal patterns in the voltage curves, while higher-order signatures (e.g., k=4) led to overfitting, particularly in scenarios with limited training data. The choice of k=3 ensures generalization and robustness across different battery groups and charging conditions.

The Toyota dataset emphasizes the impact of different charging strategies on charging curves, increasing the dataset's diversity. Given that the charging and discharging curves of electric vehicles and other battery-powered devices can be controlled in real-world applications, this study considers the charging voltage curve as one of the features for extraction. In certain cases, consistent and controlled cycling conditions are required to study the intrinsic characteristics of cells or cell-to-cell

G1 G2 G3 G4 3.5 3.5 3.5 3.5 Voltage (V) 3.0 3.0 3.0 3.0 2.5 2.5 2.5 2.0 2.0 2.0 2.0 10 10 10 5 10 Time (min) Time (min) Time (min) Time (min) G1 G2 G3 G4 3.5 3.5 3.5 3.5 Voltage (V) 3.0 3.0 3.0 3.0 2.5 2.5 2.5 15 2.0 15 2.0 2.0 10 10 10 Time (min) Time (min) Time (min) Time (min)

variations. Therefore, the discharging voltage curve is also included as a feature for extraction, as shown in Figure 1.

Figure 1: The voltage change for charging (top) and discharging (bottom)

It can be seen that the upper part shows the charging voltage curves, while the lower part shows the discharging voltage curves. Each plot displays all the cells from different groups. In the charging regime, the curves exhibit noticeable variations and fluctuations due to different charging strategies, highlighting the impact of the strategies on the charging process. In contrast, in the discharging regime, although all cells undergo the same cycling conditions, significant cell-to-cell differences are still observed in the curves. These differences are primarily due to the intrinsic properties of the cells, indicating that even under identical cycling conditions, the performance of the cells can vary.

The end-of-life for all cells used in this study is shown in the figure. The dataset covers a wide range of end-of-life values, with a minimum of 101 cycles and a maximum of 2235 cycles. Time-to-failure is determined from the capacity curves and is defined as the cycle number when the cell capacity decreases by 80% relative to its initial value. Significant differences in time-to-failure can be observed among different groups. For example, cells in groups G1 and G4 exhibit a wide range of cycle life distributions, while cells in groups G2 and G3 are all censored, with their time-to-failure truncated due to the termination of the experiment.

5.2 Parameter Configuration

5.3 Setup

We implemented a robust experimental framework to evaluate the performance of survival models for predicting the RUL of Li-ion batteries. The datasets, sourced from multiple battery manufacturers, encompass diverse battery chemistries and charging conditions. Key data attributes include battery voltage, current, capacity, and internal resistance, collected over numerous charge-discharge cycles.

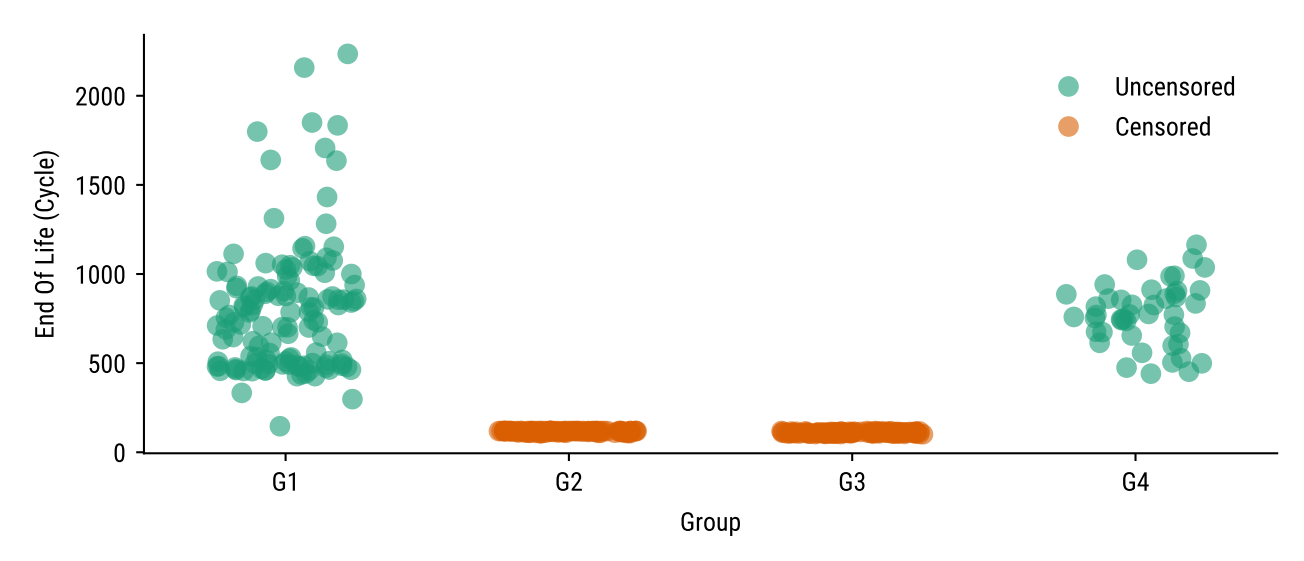


Figure 2: The distribution of time-to-failure and censorship status across different cell groups.

Experiments were conducted using an NVIDIA RTX 4070 GPU, CUDA 12.1, and Windows 11. All data were stored in CSV format. The preprocessing pipeline involved selecting the first 154 features along with event (event) and survival time (time) columns, standardizing features using Standard Scaler, and converting data to float32 using DataFrameMapper. To maintain reproducibility, the dataset was uniformly stratified into training (80%), validation (5%), and test (15%) sets with a fixed random seed (random state=10).

All models were based on a Multilayer Perceptron (MLP) architecture, with optimized configurations: Cox, CoxPH, and CoxTime used two hidden layers (64 neurons per layer), Batch Normalization, and Dropout (0.1-0.2), with Adam optimizer (lr = 0.005), batch sizes of 128-256, and Early Stopping (patience=10). CoxTime discretized survival time into 10 intervals, while Cox and CoxPH computed risk via trapezoidal integration. DeepHit and MTLR followed similar architectures with discretized survival time, using 50 and 300 epochs, respectively, with interpolation-based risk computation. Optimizations included increased network capacity (64 neurons per layer), consistent dropout (0.1-0.2) for regularization, reduced learning rate (0.01 to 0.005) for stability, and Early Stopping adjustments, ensuring robust and comparable results across all models.

5.4 Evaluation Metrics

Performance on the N test individuals $\mathbf{X} = (\mathbf{x}_1, \mathbf{x}_2, \dots, \mathbf{x}_N)$ was evaluated in terms of three independent metrics: the time-dependent AUC (T-AUC), the concordance index (C-Index) and the integrated Brier score (IBS), redefined as follows (1 is the indicator function)

• T-AUC provides a probability measure of classification ability over time. It quantifies the model's ability to address the issue "Is battery i likely to remain alive by time t?".

$$\text{T-AUC} = \frac{1}{\left|\mathcal{Z}_{0}\right| \times \left|\mathcal{Z}_{1}\right|} \sum_{i:\epsilon_{i}=0} \sum_{j:\epsilon_{j}=1} \mathbb{1}\left\{\Pr(\mathbf{x}_{i}) < \Pr(\mathbf{x}_{j})\right\}.$$

• C-Index serves as a generalization of the T-AUC, giving an estimate of how accurately the model can answer the question "Which of battery i and battery j is more likely to remain alive?".

$$\text{C-Index} = \frac{1}{\left|\mathcal{Z}_1\right|} \sum_{i \in \mathcal{Z}_1} \frac{1}{\left|\left\{j: T_i < T_j\right\}\right|} \sum_{j: T_i < T_j} \mathbb{1}\left\{\Pr(\mathbf{x}_i) < \Pr(\mathbf{x}_j)\right\}.$$

• IBS measures an ensemble prediction error across the test data, i.e., the power of a model to address the question "How accurate is the prediction that battery i will remain alive?".

IBS =
$$\frac{1}{|\mathcal{Z}_0| \times |\mathcal{Z}_1|} \sum_{i \in \mathcal{Z}_1 \cup \mathcal{Z}_0} \left(1 - \zeta_i - \Pr(\mathbf{x}_i)\right)^2.$$

5.5 Results

Table 1 compares the five models' performance, in terms of T-AUC, C-Index, and IBS, on the charging and discharging data. The Cox model demonstrates strong performance across both phases, achieving the highest T-AUC in discharge (0.932) and a competitive C-Index (0.859), indicating excellent discriminative ability. CoxTime slightly outperforms Cox in the charge phase (T-AUC: 0.919 vs. 0.909), while maintaining a comparable IBS (0.028 vs. 0.031), suggesting better overall calibration. CoxPH, a simpler proportional hazards model, lags behind both Cox and CoxTime, particularly in T-AUC (0.889 in charge, 0.896 in discharge), indicating reduced predictive power. DeepHit, a deep learning-based survival model, exhibits mixed performance. While its C-Index is relatively strong (0.823 in charge, 0.816 in discharge), its T-AUC is significantly lower (0.730 in charge, 0.866 in discharge), suggesting challenges in capturing ranking information. Additionally, DeepHit's high IBS (0.085 in charge, 0.076 in discharge) indicates poor calibration, making its probability estimates less reliable. MTLR, a flexible survival model, balances performance between ranking and calibration, achieving a strong C-Index (0.844 in charge, 0.835 in discharge) and relatively low IBS (0.040 in charge, 0.051 in discharge), making it a competitive alternative. Overall, Cox-based models (Cox, CoxTime, CoxPH) exhibit the most robust and consistent performance, particularly in T-AUC and IBS, reinforcing their effectiveness in survival analysis. DeepHit struggles with calibration despite its deep learning advantages, while MTLR provides a reasonable trade-off between discrimination and probability estimation. The results suggest that traditional survival models, particularly Cox and CoxTime, remain the most reliable choices for modeling charge and discharge survival patterns.

Figure 5 presents the change in C-Index when the models performed on the data extracted from the original data using different depth. The comparative analysis of different survival models reveals distinct performance trends across the charging and discharging datasets. Generally, Cox and CoxTime models demonstrate strong predictive capabilities, particularly in the discharging dataset, where CoxTime achieves the highest C-Index (0.862) at signature depth 3. The standard Cox model consistently improves with increasing depth, showing robust performance, particularly in discharging (0.859 at depth 4), making it a competitive alternative to CoxTime. MTLR outperforms all models in the charging dataset, achieving the highest C-Index (0.851) at depth 3, indicating its effectiveness in handling the complexities of charge-related degradation patterns. DeepHit and CoxPH models show moderate performance, with CoxPH being the weakest performer due to its lower adaptability to nonlinear dependencies. Interestingly, while most models exhibit improved performance with increasing signature depth, some models (e.g., CoxTime and DeepHit) show slight

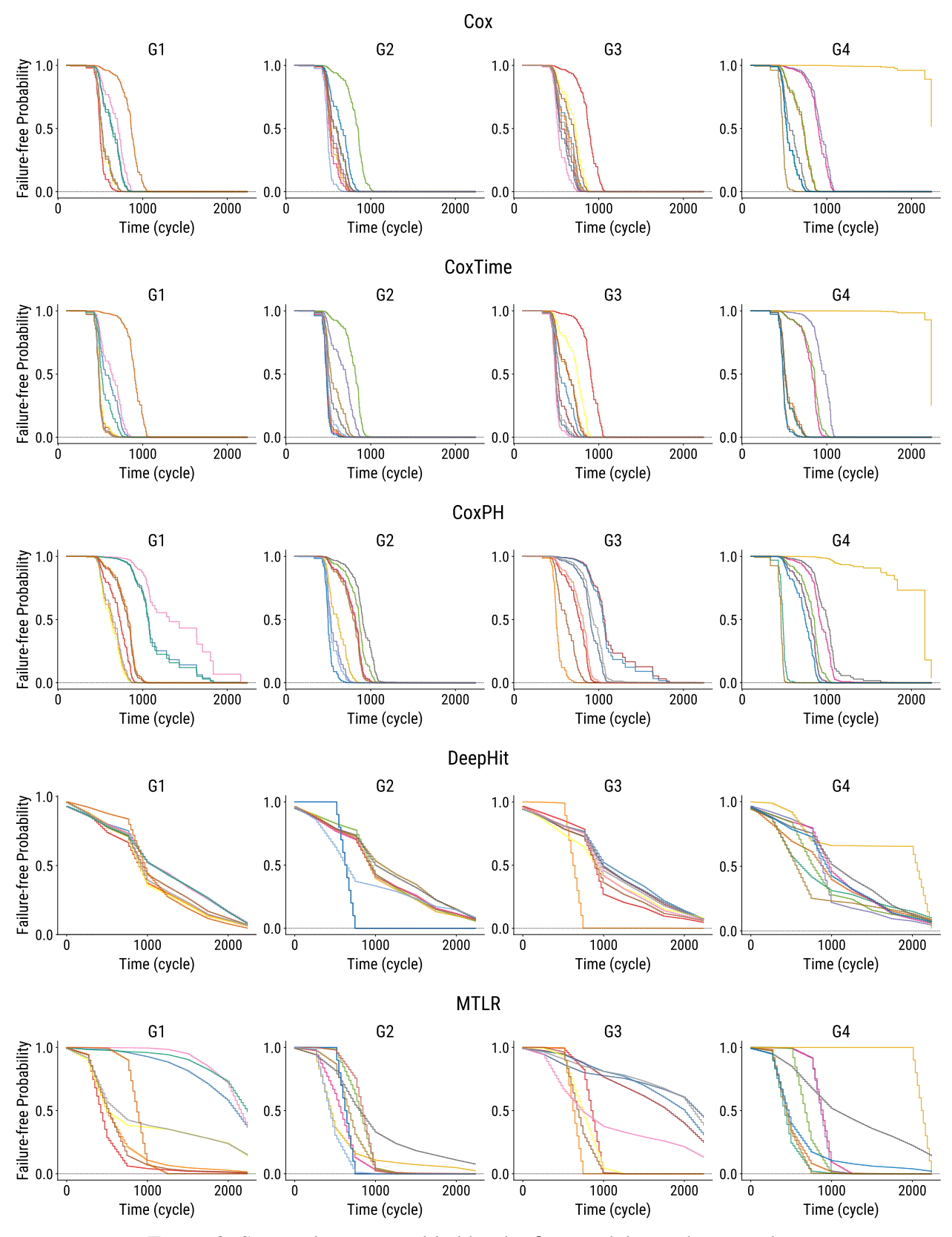


Figure 3: Survival curves yielded by the five models on charging data.

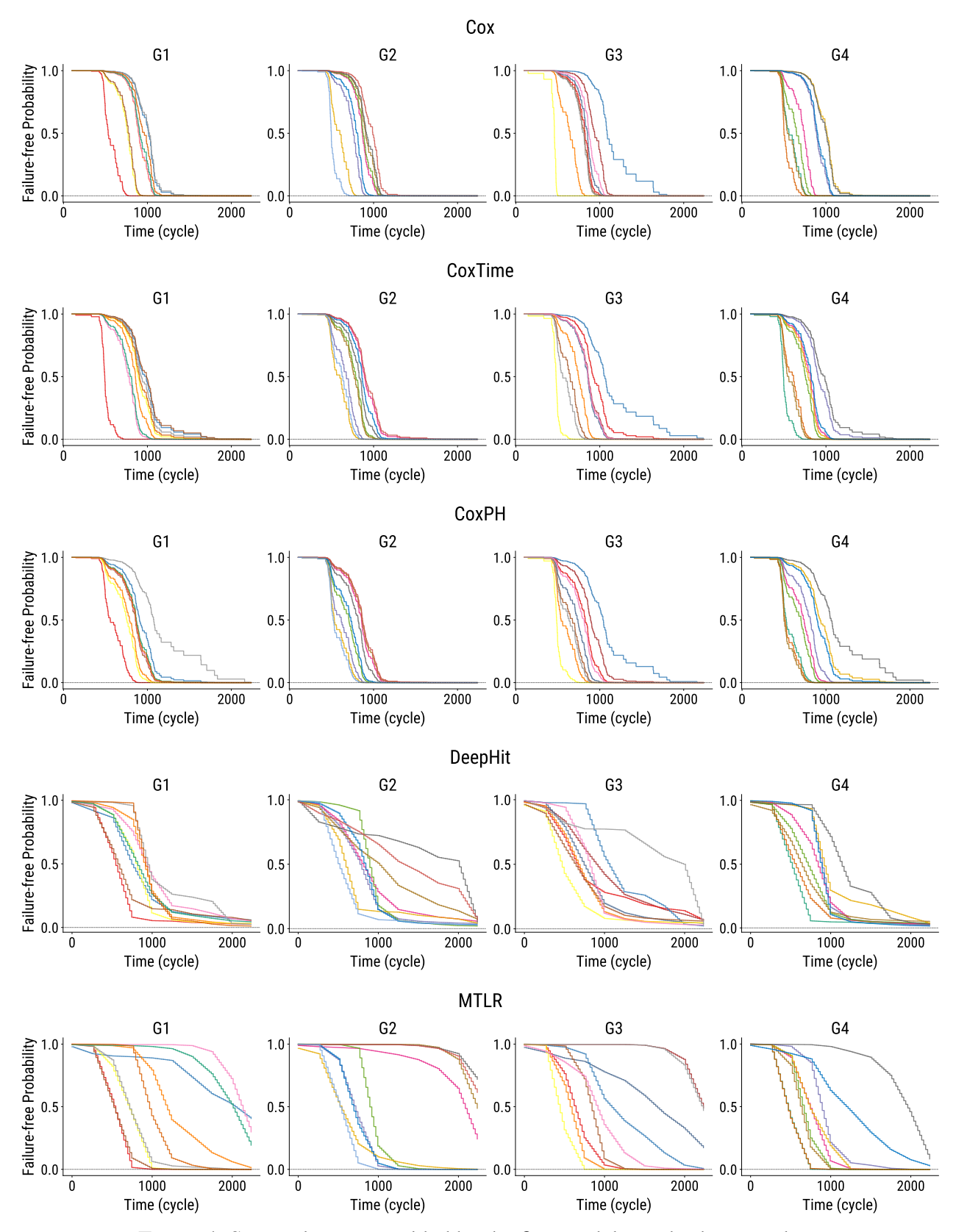


Figure 4: Survival curves yielded by the five models on discharging data.

Model	Charge			Discharge		
	T-AUC	C-Index	IBS	T-AUC	C-Index	IBS
Cox	.909(.027)	.820(.030)	.031(.006)	.932(.018)	.859(.020)	.048(.008)
CoxTime	.919(.024)	.832(.033)	.028(.006)	.929(.018)	.853(.021)	.051(.009)
CoxPH	.889(.006)	.798(.015)	.035(.001)	.896(.037)	.826(.020)	.056(.012)
DeepHit	.730(.076)	.823(.044)	.085(.012)	.866(.059)	.816(.046)	.076(.020)
MTLR	.809(.058)	.844(.024)	.040(.007)	.922(.029)	.835(.025)	.051(.009)

Table 1: Comparison of model performance, in terms of AUC, C-index, and IBS

fluctuations, suggesting sensitivity to feature complexity. Overall, CoxTime is the most effective for discharging predictions, while MTLR is the best for charging, highlighting the necessity of model selection based on specific battery operational conditions.

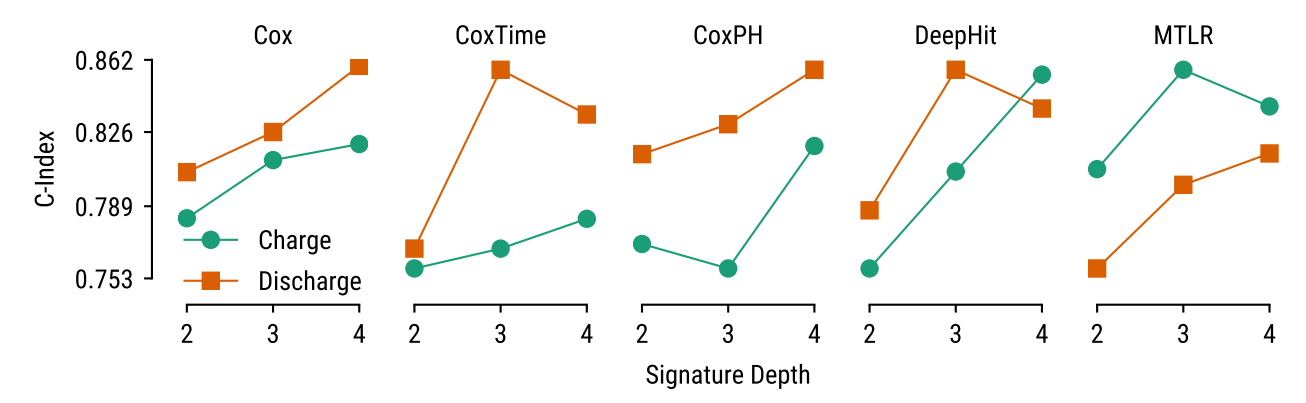


Figure 5: Comparison of models' performance on the charging and discharging data with various transformation depth.

Figure 5 shows the performance of the models when the sample fraction is changing from 25% to 100% (i.e., training set equal to test set). The analysis of five survival models - Cox, CoxTime, CoxPH, DeepHit, and MTLR - demonstrates a consistent improvement in performance as the sample fraction increases from 0.25 to 1, highlighting the positive impact of larger datasets. Among them, MTLR emerges as the most stable and high-performing model across both charging and discharging data, showing steady and reliable gains with increasing sample size. CoxTime also stands out, exhibiting significant performance jumps, especially at higher sample fractions, making it one of the strongest models when more data is available. Cox and CoxPH, while reliable, do not exhibit as steep an improvement curve as CoxTime and MTLR, though they maintain competitive performance. DeepHit, in contrast, shows more variability, with some fluctuations in results across sample fractions, suggesting it may be more sensitive to data size changes. Overall, MTLR and CoxTime are the top-performing models for survival prediction, benefiting the most from increased data, while Cox and CoxPH remain solid choices with steady improvements. DeepHit, despite improving with larger sample fractions, demonstrates more instability, making it less favorable compared to the other models.

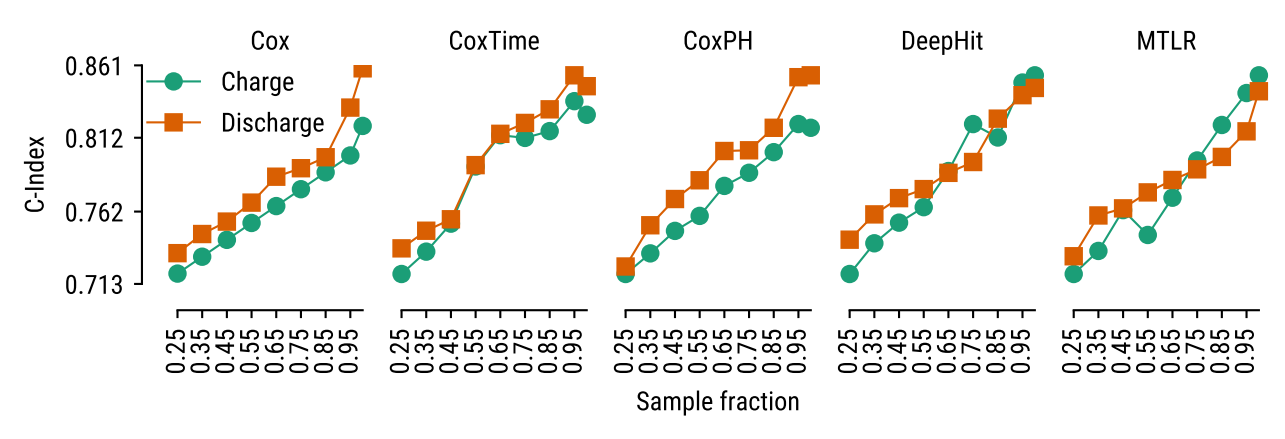


Figure 6: Comparison of models' performance on the charging and discharging data with various training and test fractions.

6 Conclusions

In this study, we proposed a novel survival analysis-based framework for predicting the RUL of Li-ion batteries. The key contributions of this work include the adoption of deep learning techniques for survival analysis, the evaluation of multiple survival models, and the assessment of their generalizability across different battery chemistries and charging conditions. We demonstrated that survival models, particularly DeepHit and Multi-Task Learning Regression (MTLR), outperform traditional models such as the Cox Proportional Hazards model in terms of both ranking accuracy and prediction precision. The MTLR model, in particular, showed excellent performance, achieving the highest C-index and lowest IBS, which indicates its strong generalization ability and robustness in real-world scenarios. Our findings highlight the potential of survival analysis in addressing the challenges of RUL prediction for lithium-ion batteries, especially in dynamic and data-scarce environments. The integration of survival models with advanced feature extraction techniques can significantly improve the accuracy and efficiency of RUL predictions, ultimately supporting the optimization of battery management systems and predictive maintenance strategies. In future work, we plan to explore additional data sources and refine our model further, incorporating more sophisticated feature engineering techniques and real-time battery monitoring data. We also aim to extend our research to other types of batteries used in various applications, such as electric vehicles and renewable energy storage systems.

References

Mohamed Ahwiadi and Wilson Wang. Battery health monitoring and remaining useful life prediction techniques: A review of technologies. *Batteries*, 11(1):31, 2025.

Maher Al-Greer, Imran Bashir, et al. Physics-based model informed smooth particle filter for remaining useful life prediction of lithium-ion battery. *Measurement*, 214:112838, 2023.

David Roxbee Cox. Partial likelihood. *Biometrika*, 62(2):269–276, 1975.

Wujin Deng, Yan Gao, Jianxue Chen, Aleksey Kudreyko, Carlo Cattani, Enrico Zio, and Wanqing Song. Multi-fractal weibull adaptive model for the remaining useful life prediction of electric vehicle lithium batteries. *Entropy*, 25(4):646, 2023.

- Bin Duan, Qi Zhang, Fei Geng, and Chenghui Zhang. Remaining useful life prediction of lithiumion battery based on extended kalman particle filter. *International Journal of Energy Research*, 44(3):1724–1734, 2020.
- Xiaosong Hu, Le Xu, Xianke Lin, and Michael Pecht. Battery lifetime prognostics. *Joule*, 4(2): 310–346, 2020.
- Jared L Katzman, Uri Shaham, Alexander Cloninger, Jonathan Bates, Tingting Jiang, and Yuval Kluger. Deepsurv: personalized treatment recommender system using a cox proportional hazards deep neural network. *BMC Medical Research Methodology*, 18:1–12, 2018.
- Mojtaba Kordestani, Mehrdad Saif, Marcos E Orchard, Roozbeh Razavi-Far, and Khashayar Khorasani. Failure prognosis and applications—a survey of recent literature. *IEEE transactions on reliability*, 70(2):728–748, 2019.
- Håvard Kvamme, Ørnulf Borgan, and Ida Scheel. Time-to-event prediction with neural networks and cox regression. *Journal of Machine Learning Research (JMLR)*, 20(129):1–30, 2019.
- Changhee Lee, William R Zame, Jinsung Yoon, and Mihaela van der Schaar. Deephit: A deep learning approach to survival analysis with competing risks. *AAAI Conference on Artificial Intelligence (AAAI)*, 32(1):2314–2321, 2018.
- De Z Li, Wilson Wang, and Fathy Ismail. A mutated particle filter technique for system state estimation and battery life prediction. *IEEE Transactions on Instrumentation and Measurement*, 63(8):2034–2043, 2014.
- Huiqin Li, Zhengxin Zhang, Tianmei Li, and Xiaosheng Si. A review on physics-informed data-driven remaining useful life prediction: Challenges and opportunities. *Mechanical Systems and Signal Processing*, 209:111120, 2024.
- Shuangzhe Liu and Gõtz Trenkler. Hadamard, khatri-rao, kronecker and other matrix products. *International Journal of Information Science and System*, 4(1):160–177, 2008.
- Baohua Mo, Jingsong Yu, Diyin Tang, and Hao Liu. A remaining useful life prediction approach for lithium-ion batteries using kalman filter and an improved particle filter. In 2016 IEEE international conference on Prognostics and Health Management (ICPHM), pages 1–5. IEEE, 2016.
- Yi Ren, Ting Tang, Quan Xia, Kun Zhang, Jun Tian, Daozhong Hu, Dezhen Yang, Bo Sun, Qiang Feng, and Cheng Qian. A data and physical model joint driven method for lithium-ion battery remaining useful life prediction under complex dynamic conditions. *Journal of Energy Storage*, 79:110065, 2024.
- MS Reza, M Mannan, M Mansor, Pin Jern Ker, TM Indra Mahlia, and MA Hannan. Recent advancement of remaining useful life prediction of lithium-ion battery in electric vehicle applications: A review of modelling mechanisms, network configurations, factors, and outstanding issues. *Energy Reports*, 11:4824–4848, 2024.
- Jiang Xing, Huilin Zhang, and Jianping Zhang. Remaining useful life prediction of—lithium batteries based on principal component analysis and improved gaussian process regression. *International Journal of Electrochemical Science*, 18(4):100048, 2023.
- Chun-Nam Yu, Russell Greiner, Hsiu-Chin Lin, and Vickie Baracos. Learning patient-specific cancer survival distributions as a sequence of dependent regressors. *Advances in Neural Information Processing Systems (NIPS)*, 24, 2011.

Jianfei Zhang, Lifei Chen, Yanfang Ye, Gongde Guo, Rongbo Chen, Alain Vanasse, and Shengrui Wang. Survival neural networks for time-to-event prediction in longitudinal study. *Knowledge and Information Systems (KAIS)*, 62:3727–3751, 2020.